Effect of Chain Unsaturation and Temperature on Oxygen Diffusion Through Lipid Membranes from Simulations

Oriana De Vos, Tanja Van Hecke, and An Ghysels

Abstract

Rafts are nanoscale ordered domains in biological membranes that are rich in saturated phospholipids. In this study, the influence of chain unsaturation and temperature on oxygen diffusion through lipid membranes is examined using advanced computational modeling. The studied phospholipids with increasing unsaturation are: 1,2-dipalmitoyl-sn-glycero-3-phosphocholine (DPPC), 1-palmitoyl-2-oleoyl-sn-glycero-3-phosphocholine (POPC), and 1,2-dioleoyl-sn-glycero-3-phosphocholine (DOPC). The unsaturation correlates with the area per lipid and the order parameter. Oxygen diffusion is found to be faster at higher temperature, and the solubility of oxygen in the membrane with respect to water decreases. Diffusion varies over a larger range across the membrane at 323 K in DPPC than in DOPC, whereas POPC has intermediate diffusivity. Oxygen diffusion in saturated lipids is faster at the membrane center and slower near the head group region than in unsaturated lipids. Oxygen solubility in DPPC is higher than in unsaturated lipids.

O. De Vos · A. Ghysels (✉)
Center for Molecular Modeling, Ghent University, Ghent, Belgium
e-mail: An.Ghysels@UGent.be

T. Van Hecke
Department of Information Technology, Faculty of Engineering and Architecture, Ghent University, Ghent, Belgium

1 Introduction

An important step in the energy supply to cells is the transport of molecular oxygen through biological membranes. These membranes can contain ordered domains that are rich in cholesterol, sphingomyelin, saturated phospholipids and membrane proteins. These nanoscale domains, called rafts, are surrounded by disordered domains. The rafts are believed to function together with integral and peripheral proteins and could play a role in signal transduction, intracellular transport, and protein sorting in these membranes [1, 2]. Both experimental [3] and computational [4] work have demonstrated that addition of cholesterol reduces the permeability of POPC phospholipid bilayers, and experimental work [5] confirms this trend for DOPC. Another characteristic of rafts is the richness in saturated lipids. In this paper, the effect of unsaturation and temperature on the permeability for oxygen are therefore investigated at the atomic scale. Because of the highly complex composition of cell membranes and the limitation of computational modeling, this study is performed on phospholipid bilayers with only one type of phospholipid. The phospholipid bilayers lack

O. Thews et al. (eds.), *Oxygen Transport to Tissue XL*, Advances in Experimental Medicine and Biology 1072, https://doi.org/10.1007/978-3-319-91287-5_64

embedded compounds that are present in the cellular environment, such as proteins, carbohydrates and ions, and they are thus not actual cell membranes. DOPC, DPPC, and POPC (Fig. 1) are selected, because these membranes have a different degree of ordering as is observed in the structure factors [6, 7]. This study is therefore a precursor to studying liquid (dis)ordered phases (L_o and L_d) [8], which are models of membrane rafts.

A DOPC molecule contains two oleic acids and a DPPC molecule two palmitic acids. Oleic acids are unsaturated with a cis double bond between carbons 9 and 10 in the tail; this introduces packing disorder in bilayers. Palmitic acids are fully saturated and pure DPPC bilayers are relatively more ordered than those with unsaturated chains [6]. POPC molecules contain one oleic and one palmitic acid, and is the more common lipid in biological membranes.

Molecular dynamics (MD) are performed at the human body temperature of 310 K for DOPC and POPC. Because the DPPC membrane is a gel at this temperature, the temperature is set to 323 K for DPPC. To allow for comparison, the DOPC and POPC membranes are also studied at 323 K.

The MD trajectories are used as input for the Bayesian analysis (BA), as presented in the Methods section. This methodology was previously developed and tested on a model mitochondrial membrane at 310 K [9]. The BA yields the free energy $F(z)$, the diffusion $D_{\perp}(z)$ normal to the membrane, and the diffusion $D_{//}(z)$ parallel to the membrane, which are shown in the Results section. These profiles give the preferred location of O_2 (F) and the anisotropy of the O_2 transport ($D_{//}$ versus $D_{\perp}$). Comparison between the five simulated systems provides insight in the effect of unsaturation and temperature on solubility and diffusion.

2 Methods

Each simulation box (Table 1) contains a phospholipid bilayer with 36 phospholipids per leaflet, a water layer, and 10 oxygen molecules (Fig. 1). Periodic boundary conditions are applied on the tetragonal box with sizes given in Table 1.

The MD simulations were performed with the CHARMM software [10] using the CHARMM36 lipid force field [11] and the modified TIP3P water model [12]. The MD simulation consists of two parts: the equilibration (NPT simulation) and the data collection (NVT simulation). Four uncorrelated snapshots of the NPT simulation were selected as the starting point for an NVT simulation of 50 ns [9].

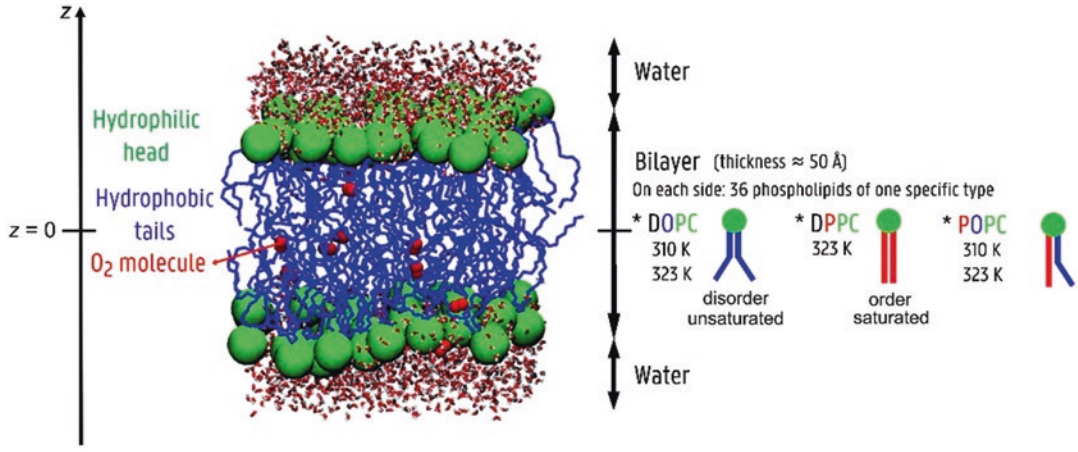

Fig. 1 Simulation box contains a bilayer (thickness ≈ 50 Å) of phospholipids, 10 oxygen molecules, and water. Phospholipids DOPC, DPPC, and POPC vary in their degree of unsaturation and order. DPPC is more ordered (higher $<S_{CD}>$ in Table 1) and DOPC is more disordered (lower $<S_{CD}>$ in Table 1)

Table 1 The five modeled systems with lipid type, temperature T, simulation box size, number of water molecules per box, area per lipid A, and plateau value $\langle S_{CD} \rangle$ of the order parameter. Each box contains 72 lipids and 10 O_2

System name	Lipid type	T (K)	$a = b$ (Å)	c (Å)	# waters	A (Å^2)	$\langle S_{CD} \rangle$
DOPC/310	DOPC	310	50.3	66.0	2409	70.4	0.179
DOPC/323	DOPC	323	50.9	65.3	2409	72.0	0.172
DPPC/323	DPPC	323	47.8	68.0	2189	63.5	0.213
POPC/310	POPC	310	48.1	67.9	2242	64.2	0.208
POPC/323	POPC	323	49.7	65.0	2242	68.6	0.188

The 200 ns data of the NVT simulation was used to determine $F(z)$, $D_\perp(z)$ and $D_{//}(z)$ for O_2. The protocol to create the profiles is based on BA of the trajectories, assuming that the Smoluchowski equation describes the oxygen diffusion in the inhomogeneous and anisotropic membrane [9, 13]. In the analysis, the coordinate of each O_2 at time t is compared to its coordinate at time $t + \tau$, while keeping track of its location in the membrane to account for inhomogeneity. The diffusion profiles depend on the studied lag time τ. The diffusion profiles with lag times 20, 30, 40 and 50 ps are fitted in order to omit the short time behavior and reach the long time scale diffusive behavior [9]. The POPC/310 system has been reported in [9], which compared them to O_2 diffusion in the inner mitochondrial membrane at 310 K. The MITO/310 system in [9] contained 10 oxygens, 72 phospholipids of various types, 2980 waters, and some ions.

The plateau value $\langle S_{CD} \rangle$ of the deuterium order parameter is calculated by averaging over the CH vectors of the C_4, C_5 and C_6 carbon atoms of both tails [6].

3 Results

3.1 General Shape of Profiles

Figure 2a plots $F(z)$ for each system, while Fig. 3 presents $D_\perp(z)$ and $D_{//}(z)$. Overall, the same trends are found for the new profiles as for the previously investigated POPC/310 and MITO/310 membranes [9]. Each system has a free energy dip at the tail region and at the center of the membrane (Fig. 2a). The dip in F is 2.5–3.5 k_BT lower than the reference at the water phase, showing the higher solubility of O_2 in fatty acids than in water, as expected [14]. In the head group region, a free energy barrier is found of approximately 1 k_BT. Comparison of $F(z)$ with the electron density (Fig. 2b) shows that the shape of $F(z)$ is largely explained by the packing density of the lipids: the greater the free volume, the higher the solubility.

Both $D_\perp(z)$ and $D_{//}(z)$ show a peak at the membrane center (Fig. 3), indicating that O_2 diffusion is fast in the interleaflet space. Near the head group region, the diffusion drops considerably. The anisotropy ratio $D_{//}/D_\perp$ shows that oxygen diffusion is faster radially in the interleaflet space and is faster normally in the tail regions (Fig. 4), which agrees with the observation for POPC/310 and MITO/310 [9].

3.2 Precision of Profiles

For each of the four studied lag times, the Monte Carlo procedure in the BA generates 1000 profiles, which are used to determine the average F, $D_\perp$ and $D_{//}$ profiles [6]. The standard deviation on these profiles is evaluated in 100 bins. The maximum standard deviation on the F values over all bins, systems, and lag times is 0.036 k_BT, which is very small compared to the F range of about 4 k_BT, and error bars are omitted in Fig. 2. The relative standard deviation for $D_\perp$ and $D_{//}$ is at most 1.2%, which is very low for diffusivities. Differences in the maximum (relative) standard deviations between the four lag times were negligible.

Moreover, the linear fit for the diffusion profile with different lag times gives a relative standard error on the intercept ($D_\perp$ or $D_{//}$). For $D_\perp$, this is on average 1.0% and at most 3.4%, taken over all systems and all bins. Since the fit is based on four lag times for each bin, the 95% confidence interval for $D_\perp$ is obtained with $t_{(0.975,2)} = 4.3$,

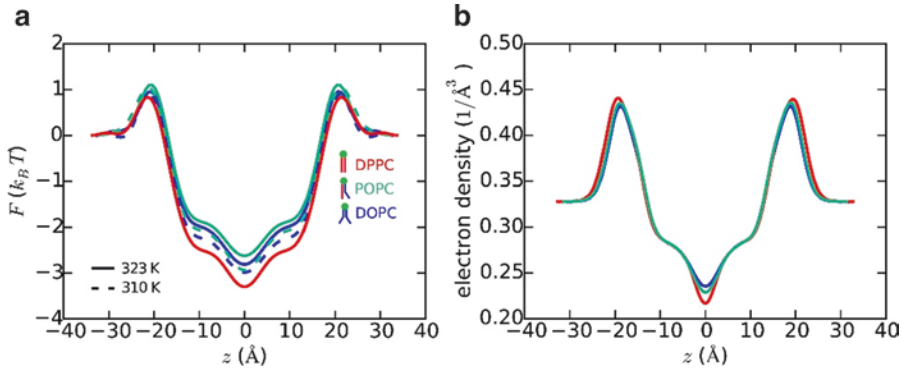

Fig. 2 $F(z)$ profile (**a**) and electron density (**b**). The oxygen concentration is proportional to the Boltzmann factor $e^{-F(z)/k_BT}$. Profiles are shifted to let the reference coincide with the water phase

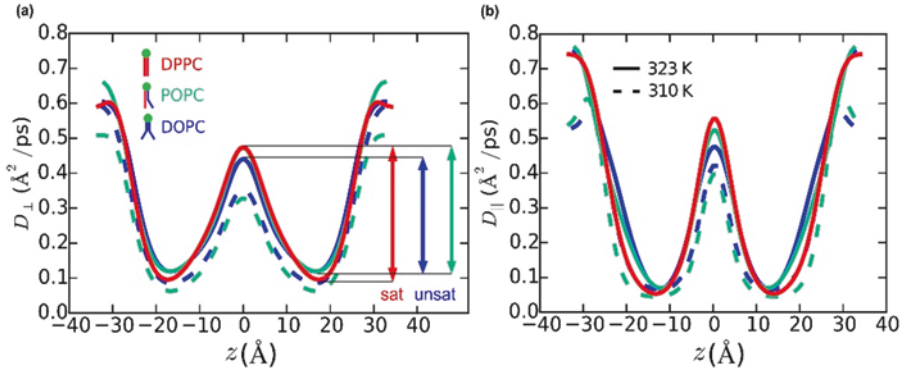

Fig. 3 $D_\perp$ profile (**a**) and $D_{//}$ profile (**b**) of oxygen diffusion. Range of D inside the membrane at 323 K is indicated with an arrow; it is larger in the saturated (sat) than in unsaturated lipids (unsat)

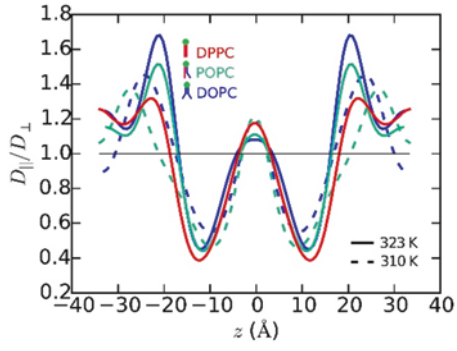

Fig. 4 Anisotropy ratio $D_{//}/D_\perp$ of oxygen diffusion

giving on average ±4.4% and a maximum of ±14.7%. The $D_{//}$ profile is less precise with a relative standard error of on average 2.8% taken over all systems and bins. This higher average is in part due to large errors near the head group region, where the steepness of the $D_{//}$ profile gives rise to apparent large variations when the profile stretches slightly along the z-axis.

Besides the statistical error associated to the BA, additional errors in the profiles can arise from low sampling, e.g. of oxygen in the water phase. Such sampling errors are not reflected in the above BA errors. The BA standard deviations are therefore an underestimation for F and D in the water and head group region, while errors in the tail region are small because of high sampling. Note that the accuracy of F in the water phase and at the barrier is limited, because O_2 spends less time in the water, giving less sampling. The water phase was nevertheless chosen as the reference point in Fig. 2a to show the relative solubility of each membrane.

3.3 Effect of Unsaturation

First, consider $F(z)$ in Fig. 2a. The F profile of DPPC has a remarkably deeper well than for the others membranes, which indicates that the solubility in the saturated lipids is higher than in unsaturated lipids. If this observation also holds for more complex ordered domains, like rafts, it would imply that ordered domains rich in saturated lipids can act as storage of oxygen. DPPC differs from DOPC and POPC because it has higher ordering with a higher plateau value $<S_{CD}>$ (Table 1). This correlates well with the denser packing (lower area per lipid in Table 1) and a more defined interleaflet space (lower electron density in Fig. 2b).

The C16 chains of DPPC are shorter than the C18 chains of DOPC. For saturated lipid chains, simulations at 320 K show that the free energy barriers in the head group regions become lower and move further apart with increasing chain length [15]. The present F profile for DPPC has also lower and more distant free energy barriers, despite having shorter chains. This shows that the presence of double bonds overrules the effect of the chain length for these PC lipids.

Second, the range of the diffusivity across the membrane is considered. In Fig. 3a, the range of $D_\perp$ at 323 K is clearly larger in the DPPC membrane than in the DOPC membrane. $D_\perp$ is higher at the center and lower near the head group region of the saturated lipids than for the lipids with two unsaturated tails. Experimentally, the effect of unsaturation on the dynamics has been measured by means of the oxygen transport parameter $W(z) \sim D(z)\mathrm{e}^{-F(z)/k_\mathrm{B}T}$ (lower F), and it was found that the incorporation of a double bond at the C9–C10 position of the alkyl chain decreases $W(z)$ at all locations z in the membrane at 45 °C [5]. By combining Figs. 2a and 3a, we can predict for DPPC that the product of the higher $\mathrm{e}^{-F(z)/k_\mathrm{B}T}$ and the higher $D_\perp$ values in the chain region indeed yields a higher transport parameter than for DOPC, thus confirming the experimental finding. POPC/323 follows the trend of the ordered DPPC/323 in the interleaflet space, and is similar to DOPC/323 near the head group region. POPC with intermediate unsaturation thus shows diffusive behavior intermediate to the saturated and unsaturated lipids. Quantitatively, unsaturation has a fairly small effect on $D_\perp$. An increase of about 25% is observed from the lowest $D_\perp$ value of the saturated system to the lowest value of the unsaturated systems.

In Fig. 3b, the range of $D_{//}$ at 323 K shows the same difference between saturated and unsaturated lipids as $D_\perp$. The $D_{//}$ profile of POPC/323 lies again between DPPC/323 and DOPC/323. The anisotropy ratio $D_\perp/D_{//}$ lies closer to 1 near the head group region in saturated lipids than in unsaturated lipids (Fig. 4). In the interleaflet space and the tail region, the opposite is observed with saturated lipids showing more anisotropy than unsaturated lipids.

3.4 Effect of Temperature

For DOPC and POPC, the O_2 solubility in the membrane with respect to the water phase decreases with increasing T, which is reflected by F being less deep at higher temperature in Fig. 2a. Given the possibly lower accuracy for F in the head group region and water, it is uncertain whether these relatively small differences are significant.

Both $D_\perp$ and $D_{//}$ increase substantially when T increases from 310 to 323 K (Fig. 3). This is in agreement with experimental observations that membrane permeability increases for POPC between 35 and 45 °C [3]. The effect of T is larger for POPC than for DOPC, with even a reduction of a factor 2 for $D_\perp$ of POPC near the head group region. Moreover, the anisotropy increases slightly at the interleaflet space due to this decrease of T (Fig. 4). In other regions the anisotropy reduces, with the ratio $D_{//}/D_\perp$ getting closer to 1.

4 Conclusion

The unsaturation and temperature are found to have an effect on oxygen solubility and diffusion through phospholipid bilayers. At 323 K, the O_2 solubility in DPPC is higher, and the range of

both $D_{\perp}$ and $D_{//}$ is larger, than in unsaturated lipids. When T decreases from 323 to 310 K, $D_{\perp}$ and $D_{//}$ decrease considerably and the O_2 solubility increases. Since the chain unsaturation correlates with the order parameter, these findings warrant further study on the effect of order in liquid ordered phases, which are rich in saturated lipids.

Acknowledgments We thank Richard Venable and Richard Pastor for technical advice and scientific discussions. The computational resources and services used in this work were provided by the VSC (Flemish Supercomputer Center), funded by the Research Foundation – Flanders (FWO) and the Flemish Government – department EWI.

References

1. Kupianen M, Falck E, Ollila S et al (2005) Free volume properties of sphingomyelin, DMPC, DPPC and PLPC bilayers. J Comput Theor Nanosci 2:401–413
2. Subczynski WK, Kusumi A (2003) Dynamics of raft molecules in the cell and artificial membranes: approaches by pulse EPR spin labeling and single molecule optical microscopy. Biochim Biophys Acta 1610:231–243
3. Widomska J, Raguz M, Subczynski WK (2007) Oxygen permeability of the lipid bilayer membrane made of calf lens lipids. Biochim Biophys Acta 1768:2635–2645
4. Dotson RJ, Smith CR, Bueche K et al (2017) Influence of cholesterol on the oxygen permeability of membranes: insight from atomistic simulations. Biophys J 112:2336–2347
5. Subczynski WK, Hyde JS, Kusumi A (1991) Effect of alkyl chain unsaturation and cholesterol intercalation on oxygen transport in membranes: a pulse ESR spin labeling study. Biochemistry 30:8578–8590
6. Venable RM, Brown FLH, Pastor RW (2015) Mechanical properties of lipid bilayers from molecular dynamics simulation. Chem Phys Lipids 192:60–74
7. Ogata K, Nakamura S (2015) Improvement of parameters of the AMBER potential force field for phospholipids for description of thermal phase transitions. J Phys Chem B 119:9726–9739
8. Sodt AJ, Logan Sandar M, Gawrisch K et al (2014) The molecular structure of the Liquid-Ordered phase of lipid bilayers. J Am Chem Soc 136:725–732
9. Ghysels A, Venable RM, Pastor RW et al (2017) Position-dependent diffusion tensors in anisotropic media from simulation: oxygen transport in and through membranes. J Chem Theory Comput 13(6):2962–2976
10. Brooks BR, Brooks CL III, MacKerell AD Jr et al (2009) CHARMM: the biomolecular simulation program. J Comput Chem 30(10):1545–1614
11. Klauda JB, Venable RM, Freites JA et al (2010) Update of the CHARMM all-atom additive force field for lipids: validation on six lipid types. J Phys Chem B 114(23):7830–7843
12. Jorgensen WL, Chandrasekhar J, Madura JD et al (1983) Comparison of simple potential functions for simulating liquid water. J Chem Phys 79(2):926–935
13. Hummer G (2005) Position-dependent diffusion coefficients and free energies from Bayesian analysis of equilibrium and replica molecular dynamics simulations. New J Phys 7(34):1–14
14. Battino R (1981) Oxygen and ozone, IUPAC Solubility Data Series, vol 7. Pergamon Press, Oxford. (ISBN 0-08-023915-3)
15. Sugii T, Takagi S, Matsumoto Y (2005) A molecular-dynamics study of lipid bilayers: effects of the hydrocarbon chain length on permeability. J Chem Phys 123(184714):1–8